Grid cell spatial tuning reduced following systemic muscarinic receptor blockade

Ehren L. Newman[1,*], **Jason R. Climer**[1], and **Michael E. Hasselmo**[1]

[1]Center for Memory and Brain, Department of Psychology, Boston University, 2 Cummington Mall, Boston, Massachusetts, 02215, U.S.A

Abstract

Grid cells of the medial entorhinal cortex exhibit a periodic and stable pattern of spatial tuning that may reflect the output of a path integration system. This grid pattern has been hypothesized to serve as a spatial coordinate system for navigation and memory function. The mechanisms underlying the generation of this characteristic tuning pattern remain poorly understood. Systemic administration of the muscarinic antagonist scopolamine flattens the typically positive correlation between running speed and entorhinal theta frequency in rats. The loss of this neural correlate of velocity, an important signal for the calculation of path integration, raises the question of what influence scopolamine has on the grid cell tuning as a read out of the path integration system. To test this, the spatial tuning properties of grid cells were compared before and after systemic administration of scopolamine as rats completed laps on a circle track for food rewards. The results show that the spatial tuning of the grid cells was reduced following scopolamine administration. The tuning of head direction cells, in contrast, was not reduced by scopolamine. This is the first report to demonstrate a link between cholinergic function and grid cell tuning. This work suggests that the loss of tuning in the grid cell network may underlie the navigational disorientation observed in Alzheimer's patients and elderly individuals with reduced cholinergic tone.

Keywords

Introduction

Grid cells in the medial entorhinal cortex (MEC) fire as a rat visits regularly spaced locations in an environment (Fyhn et al., 2004; Hafting et al., 2005; Brun et al., 2008; Hafting et al., 2008; Derdikman et al., 2009). Grid cells are embedded in a network of spatially tuned cells – sending and receiving spatially tuned activity to and from the hippocampus (van Strien et al., 2009; Zhang et al., 2013), and co-existing in the medial entorhinal cortex with cells coding for head direction and boundary proximity (Sargolini et al., 2006; Savelli et al., 2008; Solstad et al., 2008; van Strien et al., 2009; Zhang et al., 2013). The periodic spatial tuning of grid cells may provide a coordinate system for

*Corresponding author: Ehren Newman, 2 Cummington Mall, Boston, MA, 02215. Ph: 609-240-2211. enewman@gmail.com.

navigation behavior and memory formation (Moser et al., 2008), thereby serving a central role in neural information processing in healthy individuals. However, the mechanisms underlying the characteristic spatial tuning of medial entorhinal grid cells remains poorly understood.

Activation of muscarinic receptors may be critical for the generation of grid cell tuning. Muscarinic acetylcholine receptor antagonists impair navigation and memory formation (see reviews in Hasselmo, 2006; Newman et al., 2012), raising the question of what influence muscarinic antagonists have on the spatial tuning of medial entorhinal grid cells. Pharmacological inactivation of the medial septum, which sends cholinergic and GABAergic projections to the medial entorhinal cortex, results in the loss of grid tuning (Brandon et al., 2011; Koenig et al., 2011). Hippocampal recordings performed during ventricular and local administration of the muscarinic receptor antagonist scopolamine revealed that muscarinic blockade reduced the fidelity of spatial tuning and firing rates of hippocampal place cells (Brazhnik et al., 2003; 2004). Further, systemic administration of scopolamine flattens the typically robust positive correlation between running speed and theta frequency (Newman et al., 2013). Similarly, both systemic muscarinic blockade and lesions of the cholinergic cells of the medial septum reduce passive-rotation induced increases in theta power (Shin, 2010; Tai et al., 2012) indicating that cholinergic modulation is important for integrating velocity signals. Velocity signals play a critical role in computational models of grid cell tuning (for a review, see Zilli, 2012) and the loss of a velocity signal following muscarinic blockade raises the question of how muscarinic blockade would influence grid cell firing properties.

To test the hypothesis that grid tuning would be sensitive to muscarinic blockade, we compared the degree of spatial tuning of grid cells on a circle track before and after systemic scopolamine administration. We found that systemic administration of scopolamine robustly reduced the periodicity and stability of grid cell spatial tuning without significantly reducing the tuning of head direction cells.

Materials and Methods

All animal procedures and surgery were in strict accordance with National Institutes of Health and Boston University Animal Care and Use Committee guidelines.

Subjects

We recorded grid cells in 7 male Long-Evans rats: 5 were tested on circle track enclosures and 2 were tested in open field enclosures. All animals weighed 350-400 g at the time of surgery, were individually housed, were maintained at 90% of their free-feeding weight following their full recovery after surgery and maintained on a 12:12 h light-dark cycle. All procedures were conducted during the light cycle.

Surgical Procedure

For implantation of electrodes, rats were anesthetized with isoflurane and a ketamine/ xylazine mixture, the skull surface was exposed, and five to nine anchor screws and one ground screw (located anterior and lateral to the bregma skull suture) were affixed to the

skull. Tetrodes were constructed out of four 12.7 μm diameter nichrome wires twisted together that were gold plated to bring the impedance at 1 kHz down to 150-300 kΩ. Tetrodes were either bundled together and mounted in a single screw drive from Axona Ltd. or loaded into a multi-screw hyper-drive giving an average of 300 μm inter-tetrode spacing. The Axona Ltd. drive was implanted into the brain at 4.5 mm lateral, 0.3 mm anterior from the transverse sinus, 1.5 mm deep and were tilted 10 degrees in the anterior direction. The tetrode bundle of the hyper-drive was centered on a point 4.5 mm lateral and was placed anterior to the transverse sinus so that the posterior edge of the bundle abutted the sinus. No angle was used when implanting the hyper-drives. The screws and drives were attached to the skull with dental acrylic. The rats recovered for 7 days before behavioral testing and recording began.

Behavioral Protocol

The response properties of neurons were tested in an open field and on a circle track as summarized in Figure 1. The open field allowed for the identification of grid cells in all animals and was used to test the effects of scopolamine on grid tuning in two animals. Obtaining good coverage of the open field enclosure following scopolamine administration required experimenter manual intervention to coax the rats away from walls and so the circle track was used to characterize the effects of scopolamine on grid cells in the subsequent five animals. In the open field, animals foraged for cereal bits in a walled (50 cm high) rectangle enclosure (75 or 150 cm by 100 cm) as shown in Figure 1A. In the circle track task, the animals received cereal bits for each lap completed in either direction (56 cm radius; 8 cm wide track) as shown in Figure 1B. A black curtain surrounded both enclosures.

Circle track test sessions consisted of seven trials as shown in Figure 1C: pre injection screening trials on both enclosure types (trials 1 & 2); an injection trial on the circle track (trial 3); and recovery screening trials on both enclosures 3 to 6 hours and again 24 hours after the injection (trials 4 – 7). Open field test sessions consisted of four trials, all in the open field: a pre-injection screening trial; a post-injection trial; and recovery screening trials 3 to 6 hours and again 24 hours after the injection. Each trial lasted 15 min. All circle track trials were performed under low light conditions in a curtained area without overt extra-enclosure visual cues. This was done to reduce the likelihood that any loss of visual acuity following muscarinic blockade required animals to shift orienting strategy from baseline trials by minimizing the availability of visual cues in all trials.

Scopolamine Administration

Scopolamine hydrobromide injections (0.5 mg/kg) were administered intraperitoneally. This dosage was chosen because it was sufficient to generate clear changes to the tuning, fell well within the range of dosages standardly used in behavioral studies involving scopolamine and generated minimal changes to locomotor activity (0.1 – 2.0 mg/Kg) (Klinkenberg et al., 2011). Volume matched injections of sterile saline were administered as a control condition. Animals rested on a pedestal following the injection to allow for the drug to take effect before running the post-injection trial. A 30 min rest was used in open field test sessions, but this was shortened to a 15 min rest for the circle track test sessions as the behavior of the

animals suggested that the drug had taken effect by this time. A minimum of 3 intervening days was allowed between sequential scopolamine injections.

Data Acquisition

Data collection was performed with the Axona Ltd. DacqUSB system. The same system tracked the position of a large and small LED on the recording head stage to track the position and head direction of the animal at a rate of 50 Hz. Signals recorded from the tetrodes were filtered and amplified to record local field potentials (bandpass 1-250 Hz; amplified ~2,500×) and unit activity (bandpass 0.6-6.7 KHz; amplified ~8-10,000×). Potential spike waveforms were identified by a rising slope that crossed a 65-100 μV threshold and stored to disk along with a 32-bit time stamp. Spiking activity of individual units was discriminated offline using the Tint cluster cutting software (Axona Ltd., Hertz, U.K).

Data Analysis

The data analyses sought to answer the following questions: 1) Did systemic scopolamine administration change the quality of the spatial tuning of grid cells? And 2) did systemic scopolamine administration change the relationship between grid cells spiking and theta phase? The methods used to address each question are spelled out in turn.

Analyses of spatial tuning in grid cells—We sought to answer the question of whether grid tuning was reduced following systemic muscarinic blockade. In pre-injection baseline trials, the firing rate of individual grid cells varied smoothly, yet robustly, as a function of the position of the animal, generating multiple local maxima in the map of average firing rates that were positioned at consistent spatial intervals and the tuning remained stable between the first and second half of the trial. In an effort to go beyond simply saying that spatial tuning was reduced by scopolamine, we sought to characterize the influences of scopolamine on each of these tuning properties. As such, for each cell that exhibited significant grid tuning in an open field enclosure, we quantified how smooth the rate map was using the *spatial coherence* metric, how spatially periodic the rate map was using the *spatial periodicity score*, and how stable the tuning remained between the first and second half of the trial using the *tuning stability score*. Each of these metrics is described below. We then compared the observed changes to those observed following saline administration to test the significance of the observed effects.

Rate maps: Most of the metrics revolved around analysis of a firing rate map (i.e., rate map) summarizing the average firing rate for a given cell in each portion of a testing enclosure. Open field enclosurerate maps were constructed by dividing the tracked area into 3×3 cm pixels and computing the mean spike rate of each pixel. This map was then smoothed with a two-dimensional pseudo-Gaussian filter with a one pixel (3 cm) standard deviation. Circle track enclosure rate maps were computed by first linearizing the position of the animal, using the angle of the rat relative to the center of the circle, and then discretizing the track into 360 one-degree (0.9 cm) bins. This map was smoothed using a Gaussian kernel with a standard deviation of 5 degrees (4.5 cm) unless specified otherwise.

Grid cell classification: Our analyses were restricted to cells that exhibited significant grid tuning when tested in an open-field enclosure unless specifically stated. Significant grid tuning was assessed through an analyses of the grid score calculated as described elsewhere (Brandon et al., 2011). In short, we computed the correlation between the two-dimensional open field rate map autocorrelogram and a rotated version of itself for each of five different rotations (30, 60, 90, 120, 150-degrees). The correlations resulting from the 30, 90, and 150-degree rotations and from the 90 and 120-degree rotations were then compared and the smallest pairwise difference was taken to be the grid score. Individual cells were identified as grid cells if the grid score observed in the pre-injection open field screening trial was greater than 95% of the grid scores computed from a set of 200 permuted rate maps computed for that cell. Sets of permuted rate maps were computed for each cell by randomly aligning the spike times and tracking coordinates 200 times. Specifically, for each permutation, all spike time stamps were increased by a single random offset. This offset was constrained to fall between 5 and 95% of the duration of the trial. The updated time stamps, modulo the duration of the trial, were used to compute firing rate maps as described above.

Spatial coherence: The first metric sought to characterize how coherent the rate map was. During baseline recordings, the average firing rate for a given grid cell varied smoothly as a function of space, indicative that the firing rate was a product of the position of the animal. To quantify this effect, we used the spatial coherence metric (Kubie et al., 1990). In the context of this study, spatial coherence was quantified by taking the correlation between the rate map and a version of the rate map in which the firing rate at each pixel was replaced with the mean of the adjacent 10 pixels (the 5 adjacent pixels in both directions but not including itself). Importantly, this was done on a non-smoothed version of the rate map. This was repeated for epochs of clockwise and counter-clockwise running separately and the two values were linearly combined based on the percentage of time spent running in each respective direction.

Spatial periodicity score: The second metric sought to quantify the periodicity of the spatial tuning of each grid cell. Beyond having discrete fields of high- and low-firing rates, grid cells are unique in that the fields of high firing rate occur at periodic intervals. While this is particularly true in open field enclosures, periodicity is also observed on track-based enclosures such as linear tracks and the circle track used here. On the circle track, we quantified the periodicity of the spatial tuning through an analysis of the one-dimensional autocorrelation of the linearized rate map. In particular, the analysis sought to identify the presence of a secondary peak (i.e., non-zero centered) in the autocorrelation as would be observed if the rate map was self-similar to a rotated version of itself. This was accomplished by computing the correlation between the autocorrelation and a family of cosine waves, each with a different frequency, plotted from π to 3π. The result was a set of correlation values, corresponding to each of the different frequencies, with a local maximum for the frequency at which the peak aligned with the secondary peak of the autocorrelation. The correlation coefficient itself provided a quantification of the goodness-of-fit of the cosine wave and served as our metric of spatial periodicity. The spatial autocorrelation for clockwise and counter-clockwise movements were analyzed separately and the resulting scores were linearly combined based on the relative time spent moving in each direction.

Tuning stability score: The third, and final, metric of spatial tuning sought to quantify the intra-trial reliability of the spatial firing pattern. During baseline recordings, the spatial tuning of grid cells is reliable in that the cells will fire in similar locations between the first and second half of the trial. To quantify this effect, we computed the Pearson correlation coefficient between rate maps computed separately for the first and second half of the trial. The tuning stability for clockwise and counter-clockwise movements were analyzed separately and the resulting scores were linearly combined based on the relative time spent moving in each direction.

1D grid cell classification algorithm: Although all cells were positively identified as exhibiting significant grid tuning in open field enclosures, it is not known if all such grid cells code space in an analogous fashion in 1-dimensional environments. In other reports where it was not always possible to positively identify the cells as 'grid cells' as identified in 2D enclosures (Domnisoru et al., 2013; Schmidt-Hieber and Häusser, 2013) 1D grid cell classifiers have been proposed. In an effort to align our results to those reported elsewhere using 1D enclosures to explore grid tuning, we applied the classifier described by (Domnisoru et al., 2013). This allowed us to quantify, for each trial type, the number of cells that met the full set of criteria to qualify as a grid cell. Briefly, by this method, grid cells had to have at least three transitions between in-fields and out-of-fields, the widest field could not be wider that 90 cm, at least 30% of the rate map bins were either in-field or out-of-field, and the mean in-field to mean out-of-field firing rate ratio was greater than 2. In-field and out-of-field were defined based on a comparison of the rate map to the permuted rate maps (computed as described in subsection headed *Grid cell classification*) to identify portions (15 cm or longer for in-field windows, and 10 cm or longer for out-of-field windows) for which the observed firing rate differed sufficiently from the permuted values (higher than 85% of the permuted values for in-field windows, and lower than 5% of the permuted values for out-of-field windows). Readers should refer to Domnisoru et al (2013) for a full set of specifications.

Spike/theta-phase alignment—We then sought to test if the coupling between grid cell spiking and theta phase was altered by scopolamine. Grid cell firing is characteristically modulated by theta (Hafting et al., 2005; Brun et al., 2008); resulting in theta rhythmicity in the spike time autocorrelation and significant phase-locking. We tested the influence of scopolamine on each of these properties using the methods described in-turn here.

Theta rhythmic spiking: Theta rhythmic spiking of each cell was estimated using the theta rhythmicity index described elsewhere (Sharp and Koester, 2008a). In short, we computed the correlation between the smoothed spike time autocorrelation (500 ms max-lag, 1 ms bin size, smoothed with 25 ms wide boxcar) and a set of cosine waves with frequencies spanning 4 to 12 Hz in 0.01 Hz intervals and took the frequency of the wave with the highest correlation (of at least 0.164) as an estimate of the frequency of the rhythmicity. The degree of rhythmicity was calculated as the difference between the height of the first trough and first peak (i.e., the peak adjacent to the zero-centered peak) divided by the height of the first peak.

Phase locking: The degree to which the firing of each cell was locked to theta phase was calculated by computing the mean firing rate of the cell at each of 36 ten-degree phase bins and then computing the mean resultant vector of this circular histogram. The length of the vector reflected the degree of phase locking.

Down sampling—An observed effect of scopolamine administration was a reduction in the mean firing rate of grid cells. Because a number of the metrics of interest are sensitive to overall spike rate, it was important to test if the observed changes in those metrics between the pre-injection and injection trials was exclusively the result of this reduction. To do so, we replicated each analysis using a down sampled version of the observed pre-injection spike train such that the mean spike rates for the pre-injection and injection trials were matched. Down sampling was performed by randomly omitting individual spikes until the appropriate mean firing rate for the trial was reached.

Head direction tuning—Previously reports have demonstrated that grid tuning can be lost while head direction is preserved in the medial entorhinal cortex following various manipulations (Brandon et al., 2011; Koenig et al., 2011; Bonnevie et al., 2013), motivating us to explore the influence of muscarinic blockade on head direction coding in the cells recorded for this study. Individual cells were classified as exhibiting significant head direction coding if, during the open field screening trial, the Watson's U2 score for that cell was above 5. To evaluate the influence of scopolamine on the head direction tuning we compared the mean resultant length computed over headings at each spike over trials.

Statistics—Statistical comparisons focused on assessing the influence of the drug administration on each metric. As such, the pre-injection and injection trial values for each metric were contrasted in a pair-wise fashion using a paired-samples t-test. We then compared the magnitude of the differences observed following scopolamine administration to those observed following saline administration using a student's t-test for independent samples because few of the cells were well isolated throughout both the scopolamine and saline sessions.

Data inclusion criteria

Analyses were performed on cells for which the recorded data properties remained stable across the first day of the session. Three sessions were excluded because cells that were identified as grid cells in the pre-injection trials drifted such that positive identification following the injection was not possible.

Results

Overview

The results demonstrate a robust decrease in spatial tuning of the medial entorhinal grid cells following systemic scopolamine administration. Head direction tuning was not reduced, indicating that the effect was selective to grid tuning and that the animal was not completely disoriented. Additional analyses revealed a non-significant trend toward decreased theta

rhythmicity of grid cell spiking and no change in the phase-locking of grid cell spiking to theta phase.

Grid cell circle-track spatial tuning reduced by muscarinic blockade

Grid cells were identified during screening sessions in an open field testing enclosure. Once identified, the tuning properties of those cells were characterized on a circle track enclosure (summary of the full testing protocol is shown in Figure 1). Cells that had exhibited significant grid tuning during an open field trial (n = 39) showed a pattern of distinct fields of increased firing on the circle track as shown in Figure 2, similar to previous observations on linear tracks (Brun et al., 2008; Hafting et al., 2008; Derdikman et al., 2009; Domnisoru et al., 2013). Visual comparison of the circle track tuning between the baseline and scopolamine trials shows a clear decrease in spatial tuning, as shown in Figure 3. We quantified the influence of scopolamine administration on the tuning using three analyses: 1) the spatial coherence of the rate map; 2) the spatial periodicity as evidenced by the rate map autocorrelation; and 3) the intra-trial stability of the spatial tuning. Finally, we used the 1D grid cell classification algorithm described by Domnisoru et al. (2013) to assess how the percentage of cells for which the observed tuning on the circle track met the a priori criteria before, during and following the influence of scopolamine.

As expected, the spatial coherence, spatial periodicity and spatial tuning stability were relatively high during baseline trials as shown in Figure 4. The mean +/- standard deviation of the spatial coherence score was 0.55 +/- 0.03 (shown in Figure 4A), indicating that the mean spike rate at each pixel of the unsmoothed rate map was well correlated with the mean of the adjacent pixels. The periodicity score was 0.70 +/- 0.04 (shown in Figure 4B), indicating that the spatial autocorrelation had a secondary peak (i.e., a peak not centered on zero) that was strongly sinusoidal. The tuning stability score was 0.63 +/- 0.03 (shown in Figure 4C), indicating that rate maps computed separately for the first and second half of the trial were well correlated. In each of these metrics, larger values reflect greater spatial tuning while values closer to zero reflect less spatial tuning. Using the 1D grid cell classification algorithm defined by Domnisoru et al. (2013), 72% (28 or 39) of the cells that exhibited significant grid tuning in the 2D open field enclosure were classified as grid cells on the circle track (shown in Figure 4D).

During scopolamine trials, we observed significant decreases in all four metrics reflecting an overall decrease in the coherent, periodic and stable spatial tuning of the grid cells (Figure 4). The spatial coherence decreased significantly from 0.55 +/- 0.03 to 0.31 +/- 0.03 as shown in Figure 4A (p = 6e10-12, t(38) = 9.8), indicating that the firing rates of individual pixels of the rate map were less correlated with the mean of the adjacent pixels. Analysis of the periodicity revealed that the tuning observed during scopolamine trials was significantly less periodic, dropping from 0.70 +/- 0.03 to 0.42 +/- 0.04 as shown in Figure 4B (p = 6e10-8, t(38) = 10.6). Analysis of the tuning stability of the rate map during scopolamine trials indicated a significant decrease in the stability of the spatial tuning, decreasing from 0.63 +/- 0.03 to 0.43 +/- 0.03 as shown in Figure 4C (p = 1e10-15, t(38) = 13.2). The drop in tuning score likewise resulted in a significant decrease in the number cells with tuning that

was classified as being 1D grid-like by the Domnisoru et al. (2013) method as shown in Figure 4D (pre-inj trial = 72%; scopolamine trial = 28%; $p = 0.0003$, $t(38) = 4.0$).

During saline trials, no significant change was observed in any of the three metrics over the 27 cells with significant grid tuning in the open field enclosure recorded during saline sessions. The spatial coherence score was 0.49 +/- 0.05 during the baseline trials and 0.51 +/- 0.05 during the saline trials ($p = 0.44$, $t(26) = 0.8$). The tuning periodicity score was 0.66 +/- 0.05 during the baseline trials and 0.66 +/- 0.05 during the saline trials ($p = 0.99$, $t(26) = 0.02$). The tuning stability score was 0.57 +/- 0.06 during the baseline trials and 0.58 +/- 0.06 during the saline trials ($p = 0.78$, $t(26) = 0.3$). Likewise the number cells classified as exhibiting grid tuning by the Domnisoru et al. (2013) 1D grid cell classifier did not differ, (pre-inj trial = 60%; saline trial = 67%; $p = 0.54$, $t(26) = 0.6$). These results are shown in Figure 4.

The mean firing rate decreased modestly, but significantly, over cells from 1.6 +/- 0.2 to 1.3 +/- 0.2 Hz between the baseline and scopolamine trials ($p = 0.02$, $t(36) = 2.5$). This change was not significantly different from what was observed in the saline condition ($p = 0.90$, $t(64) = 0.13$). In the saline condition, the firing rate decreased from 2.0 +/- 0.3 to 1.7 +/- 0.2 ($p = 0.07$, $t(26) = 1.9$). Regardless of the similar shift in firing rate across conditions, it was important to verify that the observed changes were not a simple consequence of this change in firing rate. To do this, we down sampled the spiking during each baseline trial to match the spike rates observed during the respective injection trial. The same pattern of results was observed following the down sampling. That is, relative to baseline trials: spatial coherence was significantly lower during scopolamine trials ($p = 3\mathrm{e}10\text{-}7$, $t(38) = 6.2$), but not during saline trials ($p = 0.11$, $t(26) = 1.7$); spatial periodicity was significantly lower during scopolamine trials ($p = 2\mathrm{e}10\text{-}6$, $t(38) = 5.6$), but not during saline trials ($p = 0.95$, $t(26) = 0.1$); and the tuning stability was significantly lower during scopolamine trials ($p = 2\mathrm{e}10\text{-}4$, $t(38) = 4.1$), but not during saline trials ($p = 0.60$, $t(26) = 0.53$). These results are not shown.

Open-field scopolamine trials also show reduced spatial tuning

Our initial explorations into the influence of muscarinic blockade on grid cell spatial tuning were performed using open field enclosures during which we recorded from 6 grid cells across 2 animals. That is, the grid score was greater than 95% of the grid scores computed from a set of 200 permuted versions of the rate map. During baseline trials, the spatial tuning of these grid cells resembled the prototypical grid-tuning pattern as shown in Figure 5. Individual cells generated spikes at the vertices of a grid of equilateral triangles, yielding a mean +/- std. grid score of 0.74 +/- 0.12 (min = 0.38, max = 1.12).

The grid tuning of all 6 cells decreased robustly during scopolamine trials relative to what was observed during baseline trials. Figures 5 shows the spatial tuning of two cells before, during and after systemic scopolamine injection. During scopolamine trials, the tuning no longer resembled the grid of equilateral triangles as reflected in the decrease in the grid score in 6 of the 6 cells, from a mean of 0.74 +/- 0.12 to a mean of -0.36 +/- 0.1 as shown in Figure 6 (min = -0.70, max = -0.12; $p = 1\mathrm{e}10\text{-}5$, $t(5) = 18.1$).

As noted above, the open field enclosure data was collected prior to the circle track data described above. We stopped after collecting only six cells because both of the animals required experimenter intervention to encourage sufficient exploration of the center of the enclosure to compute the rate map. Such intervention was not necessary in pre-injection trials and was needed as a result of scopolamine induced stereotypies involving whisking along walls and corners as described previously (Schallert et al., 1980). The behavior of the animals on the circle track was much better matched between baseline and injection trials as the rats ran more consistently around the circle track. The data from these few open field sessions are included for the sake of completeness.

Grid cell theta rhythmicity and theta-phase-locking minimally reduced by muscarinic blockade

During baseline trials from circle track sessions, grid cell spiking was modestly, yet significantly, locked to theta phase as shown in a histogram of spiking over theta phases in Figure 7A. To quantify this, we computed the mean resultant length of the vectors reflecting the probability of observing a spike at each phase of theta and obtained an average value of 0.26 +/- 0.03. This magnitude of phase locking is consistent with previous reports of phase locking in the superficial layers of the medial entorhinal cortex (Mizuseki et al., 2009). During scopolamine trials, we observed a non-significant trend toward a reduction in the amount of theta phase locking (p= 0.09, t(38) = 1.8) with a mean value of 0.23 +/- 0.02. These results are shown in Figure 7C.

Consistent with the observed phase locking, the grid cell spike time autocorrelograms had multiple peaks with inter-peak intervals of about 120 ms, reflecting theta rhythmic spiking during baseline trials as shown in Figure 7B. We quantified this rhythmicity by computing the difference between the height of the first trough and the height of the first non-zero-centered peak and standardizing that difference by the height of the first non-zero-centered peak as done elsewhere (Sharp and Koester, 2008a). During baseline trials, this temporal rhythmicity score had a mean +/- std. value of 0.33 +/- 0.04. During scopolamine trials, we observed a non-significant decrease in theta rhythmicity to 0.23 +/- 0.05 as shown in Figure 7D (p = 0.11, t(38) = 1.6). Figure 7B shows the spike time autocorrelograms from the baseline trial and scopolamine trial for a single representative cell.

Head direction tuning not reduced by muscarinic blockade

Previous reports have demonstrated that it is possible to lose tuning among grid cells without reducing the tuning in head direction cells (Brandon et al., 2011; Koenig et al., 2011; Bonnevie et al., 2013) leaving open the possibility that direction information may still have been carried by these cells following muscarinic blockade. We incidentally recorded from several cells that exhibited significant head direction tuning during the open field screening trial in performing our grid cells recordings. We sought to answer the question of whether scopolamine negatively impacted the head direction tuning of these cells.

We identified 14 cells among the scopolamine condition recordings that had significant head direction tuning (Watson's U2 score > 5) during the initial open field screening trial. Two representative examples are shown in Figure 8A and 8B. The average mean resultant length

of the head direction tuning during baseline trials was 0.54 +/- 0.05. During scopolamine trials, the head direction tuning of these cells was not significantly changed (mean +/- std. = 0.53 +/- 0.06; *p* = 0.88; t(13) = 0.15) as shown in Figure 8C. Among the cells with head direction tuning, five were conjunctive grid cells in that they also exhibited significant grid tuning during the open field screening trial. The head direction tuning among these conjunctive cells was similarly preserved. Numerically, the length of the mean resultant vector during baseline trials was 0.56 +/- 0.05 and during scopolamine trials was 0.57 +/- 0.09 (*p* = 0.93; t(4) = 0.1; data not shown).

Discussion

In this report, we have shown evidence that systemic blockade of the muscarinic receptors, via I.P. injections of 0.5 mg/Kg scopolamine, reduces the spatial tuning of medial entorhinal grid cells but does not reduce the head direction tuning of cells with head direction tuning or with conjunctive head direction and grid tuning. These results offer novel insight into the mechanisms underlying the generation of grid tuning by showing the importance of cholinergic modulation via muscarinic receptors, supporting the hypothesis that acetylcholine plays an important role in tracking motion signals, and demonstrate a novel manipulation by which spatial tuning and head direction tuning can be physiologically dissociated.

Muscarinic modulation of network processing

We have shown that grid tuning was significantly reduced by the systemic administration of a muscarinic antagonist, thereby demonstrating a dependence of the grid tuning on muscarinic receptors. A number of circuit-level mechanisms exist through which muscarinic receptors may support the generation and/or maintenance of grid tuning. First, muscarinic receptors have been shown to modulate the relative strength of extrinsic versus intrinsic projections in other brain regions (Hasselmo and Bower, 1992; Linster et al., 2003; Hasselmo and McGaughy, 2004; Hasselmo, 2006; 2009). As such, blocking muscarinic receptors may diminish the relative strength of extrinsic projections into the entorhinal cortex that are required to maintain the stability or periodicity of the grid tuning. One source of such extrinsic input may be from the hippocampus. Bonnevie and colleagues (2013) have shown that hippocampal inactivation results in the loss of spatial tuning among the grid cells. Hippocampal input may provide information about spatial landmarks (Burgess et al., 2007) and/or drive a recurrent network of inhibitory interneurons that creates competition that results in the characteristic grid tuning (Burak and Fiete, 2009; Couey et al., 2013; Pastoll et al., 2013). A second circuit-level mechanism may depend upon the muscarinic receptor dependent integration properties of entorhinal neurons (Egorov et al., 2002; Fransén et al., 2006). Such integration is likely to play an important role in calibrating grid cell response to synaptic input and thus in allowing for the appropriate updating of the network state. Again, this input could be hippocampal in origin (Bonnevie et al., 2013) or provide velocity signals (Hasselmo, 2008; Hasselmo and Brandon, 2012). Third, it may be that the loss of spatial tuning observed in the grid cell population is the downstream result of a decrease in spatial tuning of hippocampus. Intracerebroventricular and intra-hippocampal

infusions of scopolamine have been shown to degrade the spatial tuning of place cells in hippocampal area CA1 (Brazhnik et al., 2003; 2004).

Motion integration and muscarinic modulation

The reduction of grid tuning observed here builds onto a growing body of evidence that cholinergic activation of muscarinic receptors is important for the sensitivity of animals to motion signals. We previously reported that systemic administration of scopolamine flattened the typically positive correlation between running speed and local field theta rhythm frequency (Newman et al., 2013). Another example comes from the demonstration that the orientation homeostasis response is lost following muscarinic blockade (Shin, 2010). That is, when mice were placed in a drum that had visually textured walls and a rotating floor, animals reflexively maintained their orientation with respect to the walls when the floor was rotated (i.e., the orientation homeostasis response). Following systemic administration of atropine (another muscarinic antagonist), this response was lost (Shin, 2010). The same results were found when the experiment was repeated in darkness (Shin, 2010) demonstrating that the reorientation is not triggered by visual input and is likely to be driven by vestibular cues. Passive whole-body rotations have also been shown to increase theta rhythm power in untreated animals (Gavrilov et al., 1995). This induced theta is attenuated by systemic muscarinic blockade in both mice (Shin, 2010) and rats (Tai et al., 2012). Again, this suggests that the blockade reduced the sensitivity of the animals to motion cues. Indeed, such desensitization to movement cues may underlie the mechanism by which scopolamine reduces motion sickness in humans (Wood, 1979). In the context of the present experiment, it may be that the loss of sensitivity to vestibular motion cues degraded the functioning of the path integration system resulting in the disruption of the grid cell tuning.

Preserved head direction tuning implies lack of complete disorientation

In the present study, we observed no significant change in the quality of the head direction tuning among the directionally tuned cells recorded despite the robust decrease in the spatial tuning among the grid cells. The preservation of head direction tuning is notable for several reasons. Most relevant for the discussion in the previous section, it indicates that the animals were not completely disoriented to allocentric direction. This raises the question of how to reconcile the apparent discrepancy between the preservation of head direction tuning seen here and the reduced sensitivity to motion signals observed previously (Shin, 2010; Tai et al., 2012). One solution may be that the previously observed reductions in sensitivity result from reduced of vestibular input whereas the intact head direction tuning observed here was preserved through the use of visual cues (Blair and Sharp, 1996; Taube, 2007; Arleo et al., 2013).

The tuning of head direction cells has been shown to be dissociable from spatial tuning in a variety of contexts (Sharp and Koester, 2008b; Brandon et al., 2011; Bonnevie et al., 2013). For example, lesions to the mammillary nulceiis sufficient to disrupt head direction tuning but leave place cell tuning intact in rats (Sharp and Koester, 2008b). Conversely, temporary inactivation of either the hippocampus (Bonnevie et al., 2013) or the medial septum (Brandon et al., 2011) disrupts the spatial tuning of grid cells but not the head direction cells

of the medial entorhinal cortex. Notably, the medial septum contains cholinergic neurons, responsible for releasing acetylcholine into the hippocampus and medial entorhinal cortex (Mitchell et al., 1982; Gorman et al., 1994). Thus, the shifts of tuning observed Brandon et al. (2011) may have been due to the loss of muscarinic receptor activation that was induced systemically in the present study.

Implications for higher function

Regardless of the mechanism by which the grid tuning was reduced, the loss of this tuning is likely to have detrimental influences on behaviors that depend on the grid signal. For example, it may be that the grid cells are required to perform spatial memory tasks in which global cues must be integrated to identify a precise intermediate location such as in the Morris water maze task. Previous studies have shown that Muscarinic receptor antagonists impair performance on variants of the Morris water maze task designed for humans (Antonova et al., 2011) and used in rats (Sutherland et al., 1982). The loss of the grid tuning may also account for the increase in disorientation that is characteristically observed in Alzheimer's patients (Henderson et al., 1989). That is, the reduced cholinergic tone that accompanies the progression of Alzheimer's disease would likely lead to the breakdown of the grid tuning and thereby may generate, or contribute to, the disorientation of the patient.

Summary

We have shown that systemic blockade of muscarinic receptors is sufficient to disrupt the spatial tuning of medial entorhinal grid cells as observed on a circle track enclosure. The head direction tuning of co-localized head direction cells was not significantly changed. These results demonstrate an important role for muscarinic modulation for grid cell tuning but not head direction tuning and may offer insight into the mechanism of disorientation observed in Alzheimer's disease patients.

Acknowledgments

References

Antonova E, Parslow D, Brammer M, Simmons A, Williams S, Dawson GR, Morris R. Scopolamine disrupts hippocampal activity during allocentric spatial memory in humans: an fMRI study using a virtual reality analogue of the Morris Water Maze. J Psychopharmacol (Oxford). 2011; 25:1256–1265. [PubMed: 20823079]

Arleo A, Déjean C, Allegraud P, Khamassi M, Zugaro MB, Wiener SI. Optic flow stimuli update anterodorsal thalamus head direction neuronal activity in rats. J Neurosci. 2013; 33:16790–16795. [PubMed: 24133279]

Blair HT, Sharp PE. Visual and vestibular influences on head-direction cells in the anterior thalamus of the rat. Behav Neurosci. 1996; 110:643–660. [PubMed: 8864258]

Bonnevie T, Dunn B, Fyhn M, Hafting T, Derdikman D, Kubie JL, Roudi Y, Moser EI, Moser MB. Grid cells require excitatory drive from the hippocampus. Nat Neurosci. 2013; 16:309–317. [PubMed: 23334581]

Brandon MP, Bogaard AR, libby CP, connerney MA, Gupta K, Hasselmo ME. Reduction of theta rhythm dissociates grid cell spatial periodicity from directional tuning. Science. 2011; 332:595–599. Internet. Available from: http://www.sciencemag.org/cgi/content/full/332/6029/595/DC1. [PubMed: 21527714]

Brazhnik E, Borgnis R, Muller RU, Fox SE. The effects on place cells of local scopolamine dialysis are mimicked by a mixture of two specific muscarinic antagonists. J Neurosci. 2004; 24:9313–9323. [PubMed: 15496667]

Brazhnik ES, Muller RU, Fox SE. Muscarinic blockade slows and degrades the location-specific firing of hippocampal pyramidal cells. J Neurosci. 2003; 23:611–621. [PubMed: 12533621]

Brun VH, Solstad T, Kjelstrup KB, Fyhn M, Witter MP, Moser EI, Moser MB. Progressive increase in grid scale from dorsal to ventral medial entorhinal cortex. Hippocampus. 2008; 18:1200–1212. [PubMed: 19021257]

Burak Y, Fiete IR. Accurate path integration in continuous attractor network models of grid cells. PLoS Comput Biol. 2009; 5:e1000291. [PubMed: 19229307]

Burgess N, Barry C, O'Keefe J. An oscillatory interference model of grid cell firing. Hippocampus. 2007; 17:801–812. [PubMed: 17598147]

Couey JJ, Witoelar A, Zhang SJ, Zheng K, Ye J, Dunn B, Czajkowski R, Moser MB, Moser EI, Roudi Y, Witter MP. Recurrent inhibitory circuitry as a mechanism for grid formation. Nat Neurosci. 2013; 16:318–324. [PubMed: 23334580]

Derdikman D, Whitlock JR, Tsao A, Fyhn M, Hafting T, Moser MB, Moser EI. Fragmentation of grid cell maps in a multicompartment environment. Nat Neurosci. 2009; 12:1325–1332. [PubMed: 19749749]

Domnisoru C, Kinkhabwala AA, Tank DW. Membrane potential dynamics of grid cells. Nature. 2013; 495:199–204. [PubMed: 23395984]

Egorov AV, Hamam BN, Fransén E, Hasselmo ME, Alonso AA. Graded persistent activity in entorhinal cortex neurons. Nature. 2002; 420:173–178. [PubMed: 12432392]

Fransén E, Tahvildari B, Egorov AV, Hasselmo ME, Alonso AA. Mechanism of graded persistent cellular activity of entorhinal cortex layer v neurons. Neuron. 2006; 49:735–746. [PubMed: 16504948]

Fyhn M, Molden S, Witter MP, Moser EI, Moser MB. Spatial representation in the entorhinal cortex. Science. 2004; 305:1258–1264. [PubMed: 15333832]

Gavrilov VV, Wiener SI, Berthoz A. Enhanced hippocampal theta EEG during whole body rotations in awake restrained rats. Neurosci Lett. 1995; 197:239–241. [PubMed: 8552308]

Gorman LK, Pang K, Frick KM, Givens B, Olton DS. Acetylcholine release in the hippocampus: effects of cholinergic and GABAergic compounds in the medial septal area. Neurosci Lett. 1994; 166:199–202. [PubMed: 8177500]

Hafting T, Fyhn M, Bonnevie T, Moser MB, Moser EI. Hippocampus-independent phase precession in entorhinal grid cells. Nature. 2008; 453:1248–1252. [PubMed: 18480753]

Hafting T, Fyhn M, Molden S, Moser MB, Moser EI. Microstructure of a spatial map in the entorhinal cortex. Nature. 2005; 436:801–806. [PubMed: 15965463]

Hasselmo ME, Bower JM. Cholinergic suppression specific to intrinsic not afferent fiber synapses in rat piriform (olfactory) cortex. J Neurophysiol. 1992; 67:1222–1229. [PubMed: 1597708]

Hasselmo ME, Brandon MP. A model combining oscillations and attractor dynamics for generation of grid cell firing. Front Neural Circuits. 2012; 6:30. [PubMed: 22654735]

Hasselmo ME, McGaughy J. High acetylcholine levels set circuit dynamics for attention and encoding and low acetylcholine levels set dynamics for consolidation. Prog Brain Res. 2004; 145:207–231. [PubMed: 14650918]

Hasselmo ME. The role of acetylcholine in learning and memory. Curr Opin Neurobiol. 2006; 16:710–715. [PubMed: 17011181]

Hasselmo ME. Grid cell mechanisms and function: contributions of entorhinal persistent spiking and phase resetting. Hippocampus. 2008; 18:1213–1229. [PubMed: 19021258]

Hasselmo ME. A model of episodic memory: mental time travel along encoded trajectories using grid cells. Neurobiol Learn Mem. 2009; 92:559–573. [PubMed: 19615456]

Henderson VW, Mack W, Williams BW. Spatial disorientation in Alzheimer's disease. Arch Neurol. 1989; 46:391–394. [PubMed: 2705898]

Klinkenberg I, Sambeth A, Blokland A. Acetylcholine and attention. Behav Brain Res. 2011; 221:430–442. [PubMed: 21108972]

Koenig J, Linder AN, Leutgeb JK, Leutgeb S. The spatial periodicity of grid cells is not sustained during reduced theta oscillations. Science. 2011; 332:592–595. [PubMed: 21527713]

Kubie JL, Muller RU, Bostock E. Spatial firing properties of hippocampal theta cells. J Neurosci. 1990; 10:1110–1123. [PubMed: 2329371]

Linster C, Maloney M, Patil M, Hasselmo ME. Enhanced cholinergic suppression of previously strengthened synapses enables the formation of self-organized representations in olfactory cortex. Neurobiol Learn Mem. 2003; 80:302–314. [PubMed: 14521872]

Mitchell SJ, Rawlins JN, Steward O, Olton DS. Medial septal area lesions disrupt theta rhythm and cholinergic staining in medial entorhinal cortex and produce impaired radial arm maze behavior in rats. J Neurosci. 1982; 2:292–302. [PubMed: 7062110]

Mizuseki K, Sirota A, Pastalkova E, Buzsáki G. Theta oscillations provide temporal windows for local circuit computation in the entorhinal-hippocampal loop. Neuron. 2009; 64:267–280. [PubMed: 19874793]

Moser EI, Kropff E, Moser MB. Place cells, grid cells, and the brain's spatial representation system. Annu Rev Neurosci. 2008; 31:69–89. [PubMed: 18284371]

Newman EL, Gillet SN, Climer JR, Hasselmo ME. Cholinergic Blockade Reduces Theta-Gamma Phase Amplitude Coupling and Speed Modulation of Theta Frequency Consistent with Behavioral Effects on Encoding. J Neurosci. 2013; 33:19635–19646. [PubMed: 24336727]

Newman EL, Gupta K, Climer JR, Monaghan CK, Hasselmo ME. Cholinergic modulation of cognitive processing: insights drawn from computational models. Frontiers in Behavioral neuroscience. 2012; 6:24. [PubMed: 22707936]

Pastoll H, Solanka L, van Rossum MCW, Nolan MF. Feedback inhibition enables theta-nested gamma oscillations and grid firing fields. Neuron. 2013; 77:141–154. [PubMed: 23312522]

Sargolini F, Fyhn M, Hafting T, McNaughton BL, Witter MP, Moser MB, Moser EI. Conjunctive representation of position, direction, and velocity in entorhinal cortex. Science. 2006; 312:758–762. [PubMed: 16675704]

Savelli F, Yoganarasimha D, Knierim JJ. Influence of boundary removal on the spatial representations of the medial entorhinal cortex. Hippocampus. 2008; 18:1270–1282. [PubMed: 19021262]

Schallert T, De Ryck M, Teitelbaum P. Atropine stereotypy as a behavioral trap: a movement subsystem and electroencephalographic analysis. J Comp Physiol Psychol. 1980; 94:1–24. [PubMed: 7189526]

Schmidt-Hieber C, Häusser M. Cellular mechanisms of spatial navigation in the medial entorhinal cortex. Nat Neurosci. 2013; 16:325–331. [PubMed: 23396102]

Sharp PE, Koester K. Lesions of the mammillary body region alter hippocampal movement signals and theta frequency: implications for path integration models. Hippocampus. 2008a; 18:862–878. [PubMed: 18702112]

Sharp PE, Koester K. Lesions of the mammillary body region severely disrupt the cortical head direction, but not place cell signal. Hippocampus. 2008b; 18:766–784. [PubMed: 18446828]

Shin J. Passive rotation-induced theta rhythm and orientation homeostasis response. Synapse. 2010; 64:409–415. [PubMed: 20034015]

Solstad T, Boccara CN, Kropff E, Moser MB, Moser EI. Representation of geometric borders in the entorhinal cortex. Science. 2008; 322:1865–1868. [PubMed: 19095945]

Sutherland RJR, Whishaw IQI, Regehr JCJ. Cholinergic receptor blockade impairs spatial localization by use of distal cues in the rat. J Comp Physiol Psychol. 1982; 96:563–573. [PubMed: 7119176]

Tai SK, Ma J, Ossenkopp KP, Leung LS. Activation of immobility-related hippocampal theta by cholinergic septohippocampal neurons during vestibular stimulation. Hippocampus. 2012; 22:914–925. [PubMed: 21542057]

Taube JS. The Head Direction Signal: Origins and Sensory-Motor Integration. Annu Rev Neurosci. 2007; 30:181–207. [PubMed: 17341158]

van Strien NM, Cappaert NLM, Witter MP. The anatomy of memory: an interactive overview of the parahippocampal-hippocampal network. Nat Rev Neurosci. 2009; 10:272–282. [PubMed: 19300446]

Wood CD. Antimotion sickness and antiemetic drugs. Drugs. 1979; 17:471–479. [PubMed: 467277]

Zhang SJ, Ye J, Miao C, Tsao A, Cerniauskas I, Ledergerber D, Moser MB, Moser EI. Optogenetic dissection of entorhinal-hippocampal functional connectivity. Science. 2013; 340:1232627. [PubMed: 23559255]

Zilli EA. Models of grid cell spatial firing published 2005-2011. Front Neural Circuits. 2012; 6:16. [PubMed: 22529780]
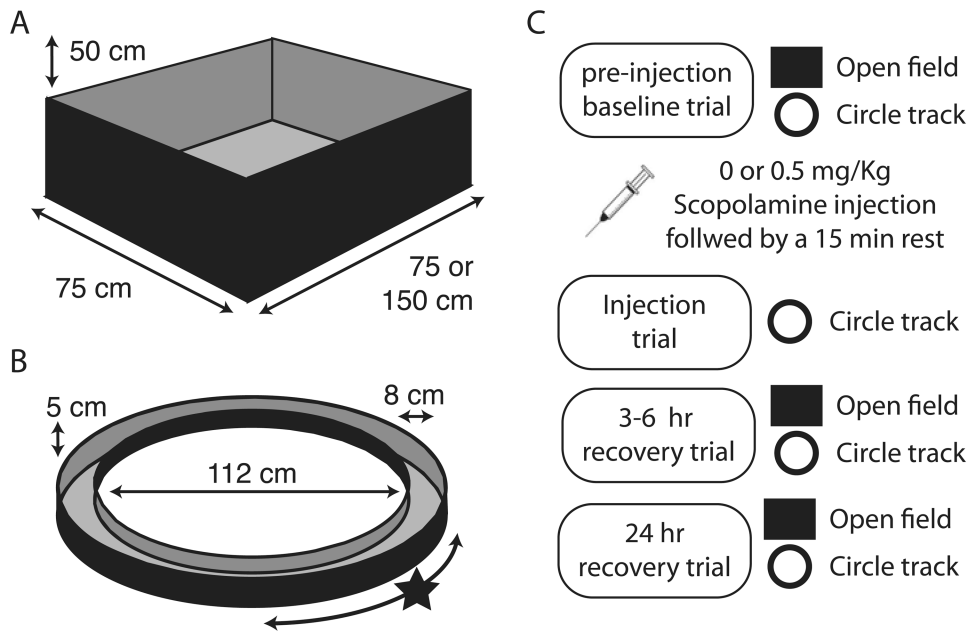
Figure 1.
Overview of apparatus and testing protocol. A. Open field (OF) testing enclosures were used to identify cells with significant grid tuning. While in the open field, animals foraged for scattered cereal bits. B. Once identified, the spatial tuning properties of those cells were tested on a circle track (CT) for *circle track sessions*. While on the circle track, animals were rewarded with cereal bits for complete laps in either direction at a fixed location (marked with a star). C. A testing session consisted of seven fifteen-minute trials: a trial on the OF and CT prior to the injection, a CT trial 15 minutes following the injection, and recovery trials on the OF and CT 3-6 hr and 24 hr post injection. Only the data from the CT trials were compared with the injection trial data.
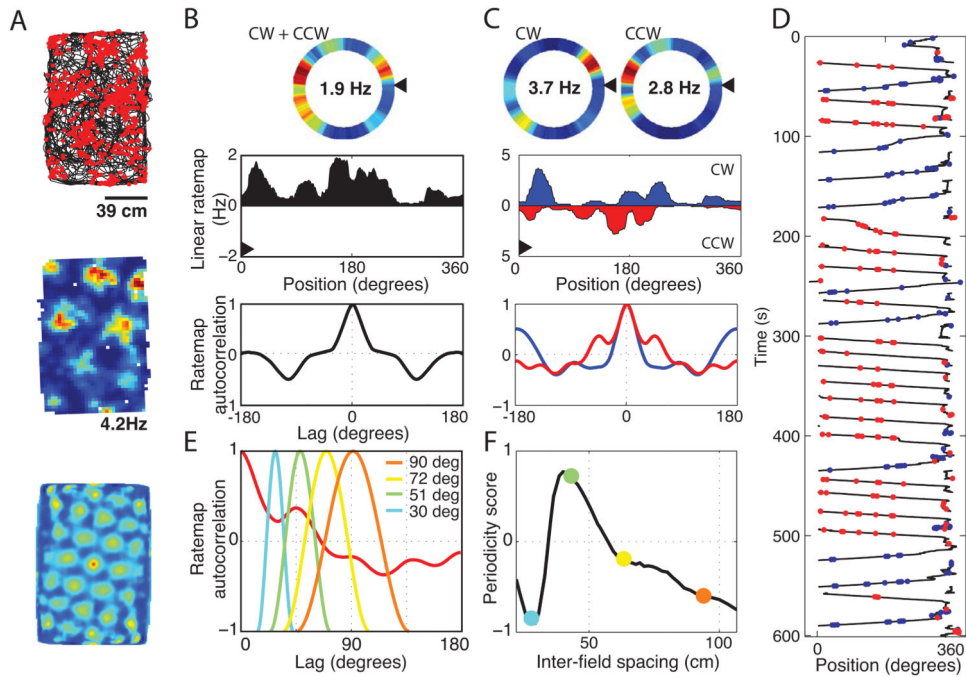
Figure 2.
Grid cell tuning on a circle track. A. Cells were identified as grid cells during the pre-injection baseline open field screening trial as cells with multiple regularly spaced firing fields that resulted in a grid score that was larger than 95% of 200 randomly permuted rate maps. The firing of a representative grid cell is shown as red dots plotted over a black line tracing the trajectory of an animal in one such screening trial (top). The rate map and 2D autocorrelogram are also shown, illustrating the standard tessellating grid structure of the spatial tuning (middle and bottom). B. The tuning of the same grid cell is shown on the circle track both as a heat-map (top). The same data is plotted as a line graph (middle) such that the leftmost edge of the line graph starts at the black arrowhead in the top graph and wraps around the circle in a counter-clockwise direction. Multiple distinct fields of high firing rate can be seen separated by fields of low firing rates. The 1D spatial autocorrelogram is shown (bottom). C. The tuning becomes more clear in this example when running is split into clockwise (CW) and counter clockwise (CCW) laps. All subsequent analyses were computed separately on CW and CCW laps and then linearly combined based on the percentage of time spent running in each direction. D. Spiking raster for the same cell. Spikes from CW laps are shown in red, spikes from CCW laps are in blue. E. The spatial periodicity of the firing rate was calculated by computing the correlation between the 1D autocorrelogram and a family of partial cosine waves of differing spatial frequencies. F. The highest correlation obtained over the set of cosine waves (as shown in E) was taken as the spatial periodicity score. The colored dots reflect the periodicity scores resulting from the analysis of the sample waveforms shown in E.
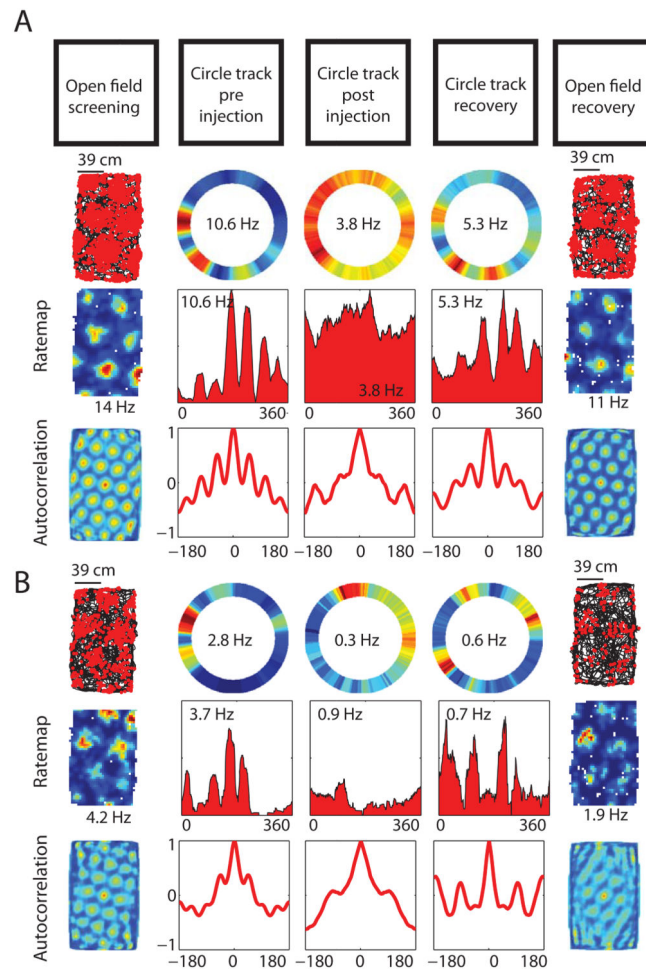
Figure 3.
Grid cell periodic spatial tuning on the circle track is reduced following scopolamine administration. A & B. Spatial tuning of two representative grid cells shown in the pre-injection open field screening trial (left column) and on the circle track before and after the systemic scopolamine injection (2nd and 3rd columns) showing a reduction in the spatial periodicity of the firing following the injection. The tuning 6 hrs after the injection are shown (4th - 5th columns) to reflect the recovery of the spatially periodic tuning.
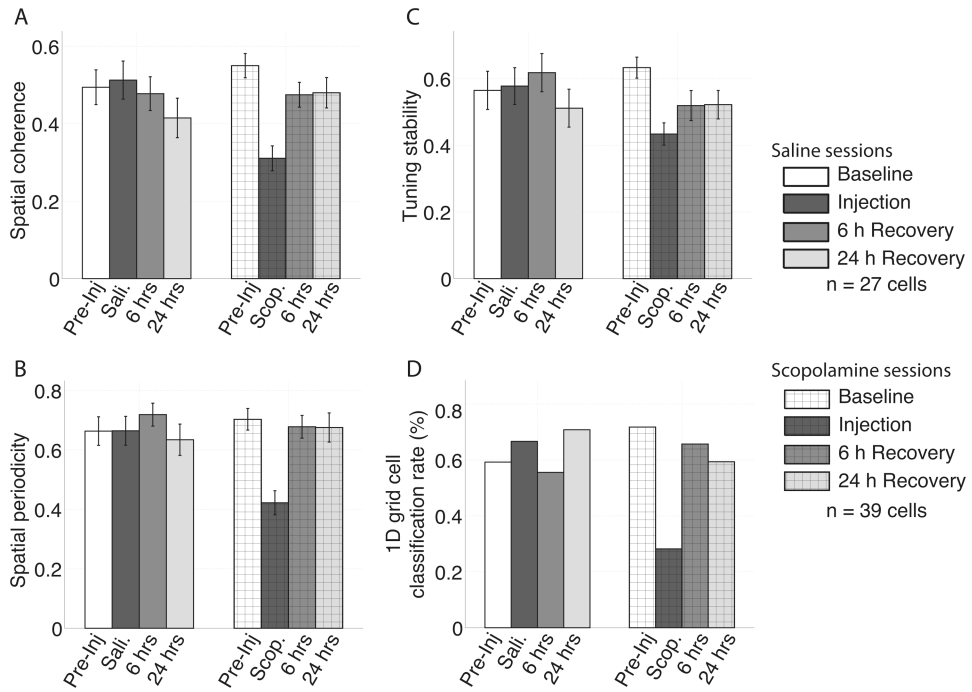
Figure 4.
Quantification of the reduction in the spatial tuning of the grid cells between the pre-injection baseline trial (pre-inj.) and the scopolamine trial (scop.) as measured by spatial coherence (A), sptial periodicity (B), and tuning stability (C). The errorbars in A-C reflect standard errors on the mean. There was no significant change between the pre-inj. trial and the saline (sali.) trial for any of the metrics. D. The percentage of cells that were classified as grid cells using the 1D grid cell classification algorithm (see methods) was robustly lower during scop. trials relative to the pre-inj. percentage.
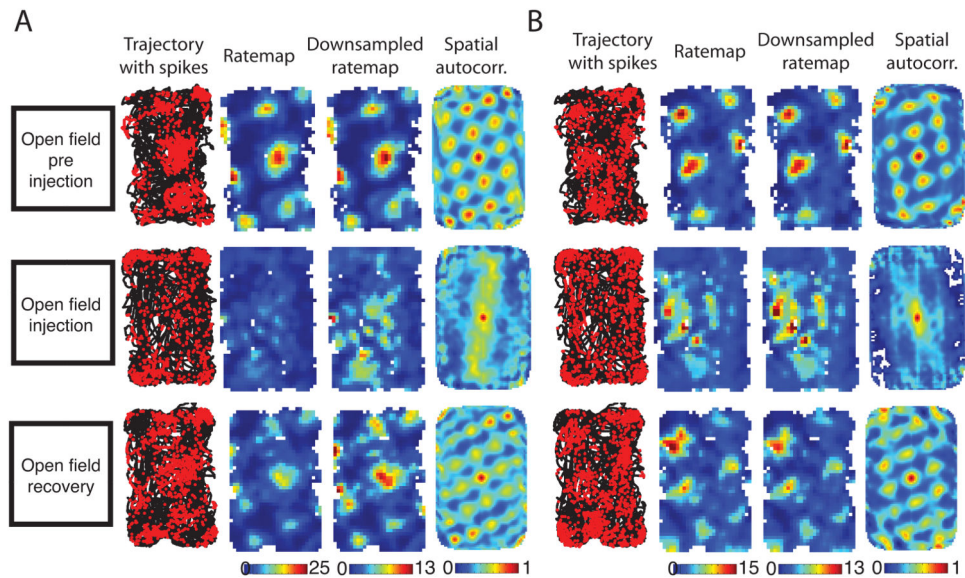
Figure 5.
Spatial tuning of two example grid cells run in open field sessions for the baseline, injection and recovery trials (A & B). For each cell, a trajectory is plotted in black with red dots indicated the location of the rat when the cell spiked. From this data a rate map was plotted that reflects the average number of spikes generated per second of dwell time at each 3×3cm pixel spanning the enclosure. The colorbar was scaled to the peak firing rate over trials. A second rate map is computed after downsampling the spiking of the baseline and recovery trials to match the trial average of the injection trial, shown as the 'downsampled rate map'. Finally, the 2D spatial autocorrelation of the rate map is shown to emphasize the self-similar repeating nature of the tuning pattern. These cells exemplify the reduction in grid-like tuning observed during the scopolamine injection trials. The effect is most visible in the loss of the grid pattern in the spatial autocorrelation during the injection trial. The grid pattern is largely restored by the time of the recovery trial 6 hrs after the injection.
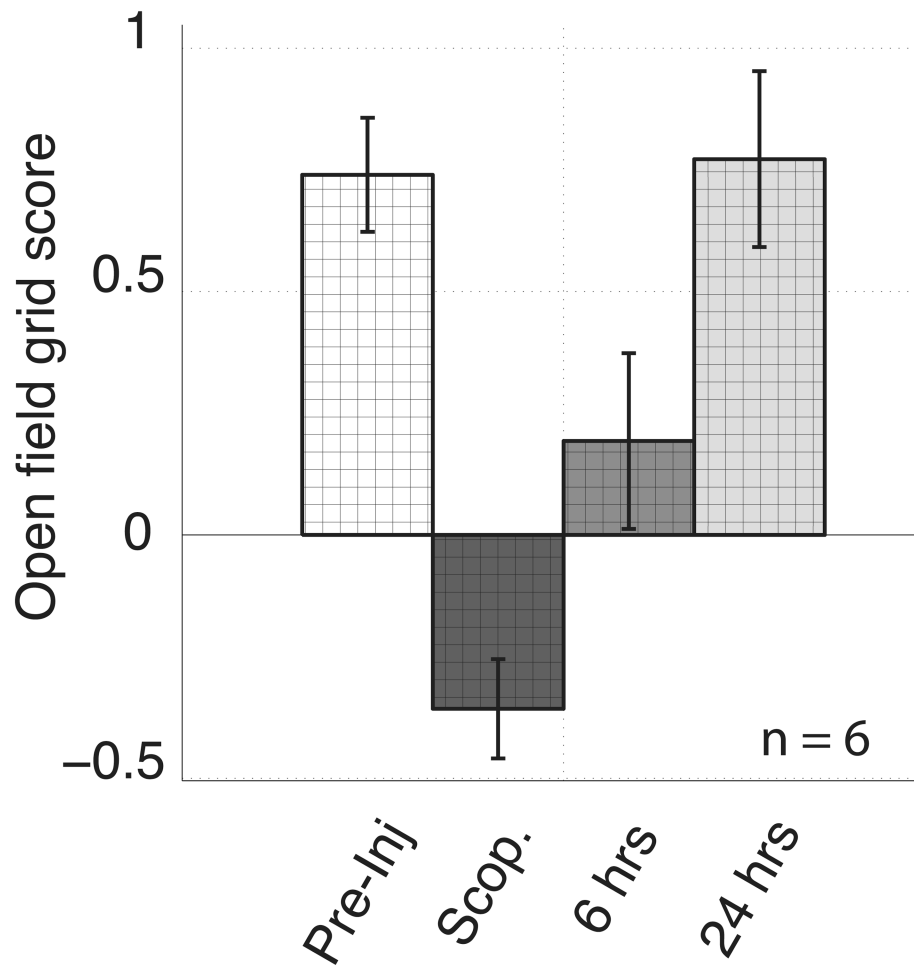
Figure 6.
Scopolamine administration significantly decreased the grid score when tested in open field enclosures. Error bars reflect standard error on the mean.
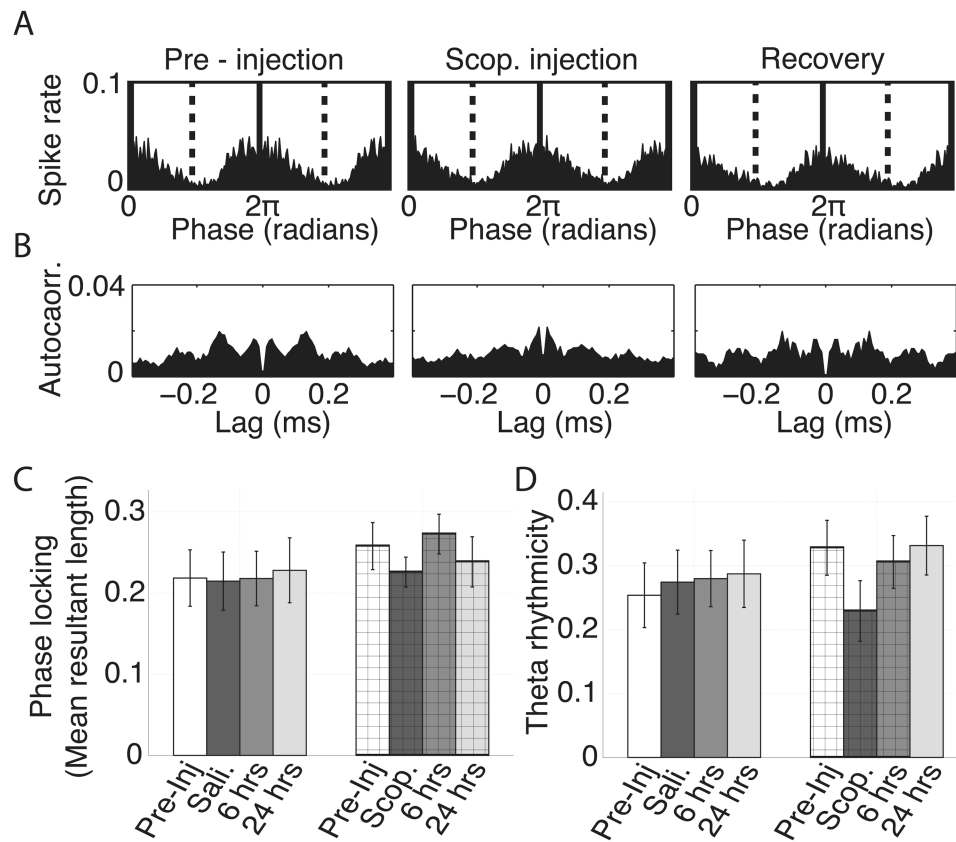
Figure 7.
Theta rhythmic spiking modestly reduced following scopolamine administration. A. Phase locking histograms for a representative grid cell, plotting the mean spike rate at each phase of theta, for the pre-injection, scopolamine and 6 hour recovery trials. Little change is observable. B. Standardized spike time autocorrelation for the same cell as shown in A showing theta rhythmic spiking in all three trial types. A modest reduction in theta rhythmicity can be seen during the scopolamine trial by the reduced difference between the standardized spike rate at 0.06 and 0.12 s, corresponding to the half and full period of a theta cycle. C. Average phase locking observed over trials for both the saline and scopolamine conditions as quantified by mean resultant length of the phase locking histograms (as shown in A). No significant differences were observed over trial types in either condition. D. Average theta rhythmicity over trials in both conditions. A trend toward a decrease can be seen between the pre-injection and baseline trials. Error bars on C and D reflect standard error on the mean.
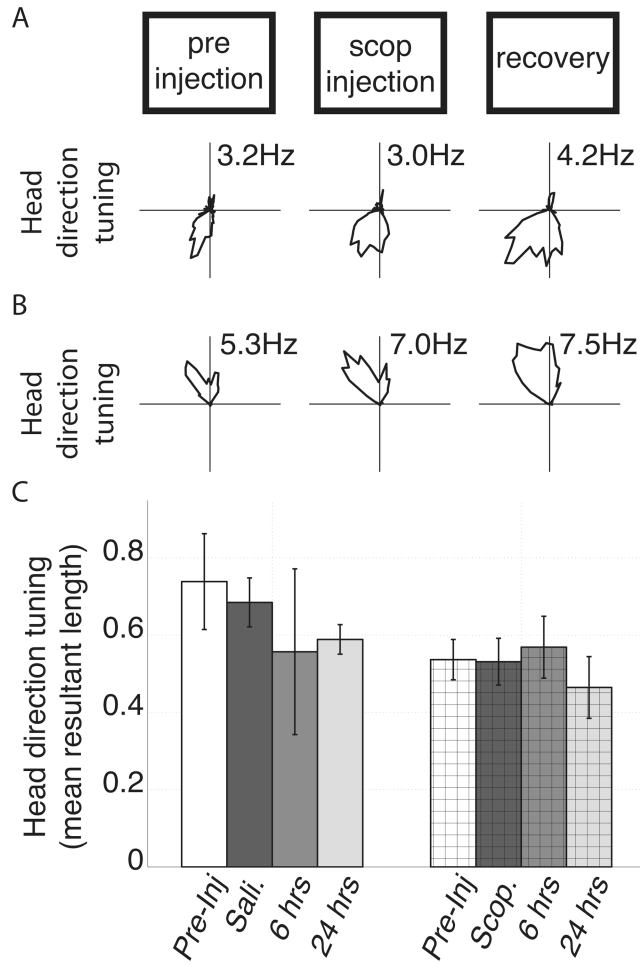
Figure 8.
Effects of saline and scopolamine administration on head direction tuning (HD tuning) of cells with significant HD tuning in the pre-injection trial. A & B. Representative tuning curves from two cells with significant head direction tuning in the pre-injection trial over trials. No difference was observed between the pre-injection and scopolamine (scop.) trials. C. Average head direction tuning of cells identified as having significant head direction tuning in the pre-injection trial over trials in both the saline and scopolamine conditions as quantified by mean resultant length of the polar rate map (as shown in A and B). We did not observe significant changes between pre-injection and injection trials in either condition. Errorbars reflect standard error on the mean.